


# Spatio-Temporal Evolution of Fogwater Chemistry in Alsace

Dani Khoury<sup>1,2</sup>, Maurice Millet<sup>1,\*</sup>, Yasmine Jabali<sup>2</sup>, Thomas Weissenberger<sup>3</sup> and Olivier Delhomme<sup>1,4</sup> 

<sup>1</sup> UMR 7515 Group of Physical Chemistry of the Atmosphere, Institute of Chemistry and Processes for Energy, Environment and Health (ICPEES), University of Strasbourg, 25 Rue Becquerel, CEDEX 3, 67087 Strasbourg, France; dani.khoury@u-bordeaux.fr (D.K.); olivier.delhomme@univ-lorraine.fr (O.D.)

<sup>2</sup> Environmental Engineering Laboratory (EEL), Faculty of Engineering, University of Balamand, Kelhat-El Koura, Tripoli P.O. Box 100, Lebanon; yasmine.jabaly@balamand.edu.lb

<sup>3</sup> Faculty of Chemistry, University of Strasbourg, 1 Rue Blaise Pascal, 67000 Strasbourg, France; tweissenberger@unistra.fr

<sup>4</sup> UFR Sciences Fondamentales et Appliquées, University of Lorraine, Rue du General Deslestraint, 57070 Metz, France

\* Correspondence: mmillet@unistra.fr; Tel.: +33-(0)368-852-866

**Abstract:** For the current article, forty-two fogwater samples are collected at four sites in Alsace (Strasbourg, Geispolsheim, Erstein, and Cronenbourg) between 2015 and 2021, except 2019 and 2020. Spatio-temporal evolution is studied for their inorganic fraction (ions and heavy metals), and physico-chemical properties (pH, conductivity (K), liquid water content (LWC), and dissolved organic carbon (DOC)). The analyses show a remarkable shifting in pH from acidic to basic mainly due to the significant decrease in sulfate and nitrate levels. The calculated median LWC is somehow low (37.8–69.5 g m<sup>3</sup>) in fog samples, preventing the collection of large fog volumes. The median DOC varies between 14.3 and 24.4 ppm, whereas the median conductivity varies from 97.8 to 169.8 μS cm<sup>-1</sup>. Total ionic concentration (TIC) varies from 1338.3 to 1952.4 μEq L<sup>-1</sup>, whereas the total concentration of metals varies in the range of 1547.2 and 2860.3 μg L<sup>-1</sup>. The marine contribution is found to be negligible at all sites for the investigated elements. NH<sub>4</sub><sup>+</sup>, in most samples, is capable alone to neutralize the acidity. On one hand, NH<sub>4</sub><sup>+</sup>, Ca<sup>2+</sup>, NO<sub>3</sub><sup>-</sup>, and SO<sub>4</sub><sup>2-</sup> are the dominant ions found in all samples, accounting for more than 80% of the TIC. On the other hand, Zn and Ni are the dominant metals accounting for more than 78% of the total elemental concentration. Heavy metals are found to primarily originate from crust as well as human-made activities. The median concentrations of individual elements either decrease or increase over the sampling period due to the wet deposition phenomenon or weather conditions. A Pearson analysis proves some of the suggested pollutant sources due to the presence of strong and significant correlations between elements.

**Keywords:** ions; heavy metals; Strasbourg metropolitan; Pearson analysis



**Citation:** Khoury, D.; Millet, M.; Jabali, Y.; Weissenberger, T.; Delhomme, O. Spatio-Temporal Evolution of Fogwater Chemistry in Alsace. *Air* **2024**, *2*, 229–246. <https://doi.org/10.3390/air2030014>

Academic Editor: Ling Tim Wong

Received: 27 May 2024

Revised: 2 July 2024

Accepted: 4 July 2024

Published: 9 July 2024



**Copyright:** © 2024 by the authors. Licensee MDPI, Basel, Switzerland. This article is an open access article distributed under the terms and conditions of the Creative Commons Attribution (CC BY) license (<https://creativecommons.org/licenses/by/4.0/>).

## 1. Introduction

Fog is a near-surface cloud in the lower atmosphere that comprises a mixture of small water droplets in the liquid form or particles suspended in the atmosphere, hindering the visibility below one kilometer [1]. It is a highly complex and dynamic system that facilitates the re-organization and removal of atmospheric pollutants [2]. The chemistry of fog depends on the sources, formation processes, and pathways of these particles in moist air; their dissolution in the aqueous phase; their reactivity; and their subsequent evaporation and surface deposition.

Fog is able to scavenge inorganic and organic species derived from hygroscopic particles and water-soluble trace gasses. Fog droplets form on aerosol particles in a super-saturated atmosphere due to combined effects of weather factors (like relative humidity, wind, temperature, pressure, etc.) and pollution (presence of aerosols) [3]. Radiation fog, which commonly occurs in Alsace, typically forms at night under stable weather conditions, characterized by clear skies and light winds. It tends to dissipate as the morning progresses

and the ground warms up due to increased thermal radiation. This type of fog is frequently observed in continental climates during winter under anticyclonic conditions, associated with high-pressure systems. Its formation begins when heat absorbed by the Earth's surface is radiated into the atmosphere, causing the ground to cool and leading to a temperature inversion. As the cooled surface releases heat, it creates a layer of moist air near the ground that reaches its dew point. This results in condensation, leading to the formation of fog [4].

Fog acts as a reservoir for the formation of new particles through the aqueous phase reactions. It may also act as a natural cleaner of the lower atmosphere through the wet deposition phenomena [5–12]. The formation of fog is facilitated not only in areas characterized by their high loadings of pollutants but in remote areas affected by the long-range transport (LRT) of pollutants from nearby sites and regions as well [13–16]. However, researchers found that fog occurrence is decreasing in Europe, which is mainly related to the amelioration in air quality, in particular the decrease in nitrate and sulfate levels [7,17–19]. For these reasons, fogwater chemistry has become a critical topic for investigation over the past few decades. The multi-dimensional characterization of fog is important for the identification of pollutant sources in the region. In-depth analyses of its sources are a major path to create some management methods to ameliorate the air quality and limit its formation and negative consequences on humans' health and the ecosystem.

Field research concerning fog chemistry has been initiated since the 1900s [20] and has received more consideration since the 1980s [11]. At the beginning of the 1990s, the first urban radiation fog samples were collected in the Alsace region during winter 1990/1991 at Strasbourg. The measurements were continued until 1999 to study the evolution of fog chemistry [21]. The investigations of such field studies at Strasbourg have been well detailed and previously reported in many scientific papers [21–25]. After that, fog studies are not sufficiently performed compared to the international assessment and evolution of the fog research [26]. Since 1999, there has been a lack of fog knowledge in the Strasbourg metropolitan area and a complete absence of fog studies. This highlights the importance of restarting fogwater collection to rebuild a robust foundation for air quality analyses, not only in France but also as a case study for global environmental monitoring. By focusing on the Alsace region, we can assess the effectiveness of environmental regulations and policies over time. These findings can offer valuable insights and methodologies applicable to other regions worldwide, contributing to the broader discourse on air quality and regulatory impacts. Fog collection was resumed in winter 2015 to study its evolution until winter 2021 at different sampling locations in the Alsace region (Strasbourg, Geispolsheim, Erstein, and Cronenbourg). So far, a recent investigation has been published concerning the analysis of polycyclic aromatic hydrocarbons (PAHs) and polychlorinated biphenyls (PCBs) [27]. In the current work, fogwater samples are analyzed for their inorganic species (heavy metals and ions) and their physico-chemical properties (pH, dissolved organic carbon (DOC), liquid water content (LWC), and conductivity (K)) at the same sites and years. It intends to investigate the following specific questions: What are the dominant ions and metals? Have their concentrations increased or decreased over time (evolution vs. time)? What are the probable sources of pollutants that influence fog chemistry based on different source identification techniques, and how does fog microphysics affect its chemical composition?

## 2. Materials and Methods

### 2.1. Studied Region

The area under study is situated in northeastern France, and it is bordered by Lorraine to the west and Franche-Comté to the southwest, Switzerland to the south, and Germany to the east and north. Alsace is known for its chemistry laboratories, extensive industrial and mining history, and agro-food industries. It has a semi-continental climate at low altitudes and a continental climate at high altitudes, characterized by cold, dry winters and hot, stormy summers. The average annual temperature is 10.4 °C (51 °F) in the lowlands (Entzheim) and 7 °C (45 °F) on high ground. The annual precipitation is relatively low, ranging from 500 to 700 mm (20 to 28 inches). The Alsace region experiences radiation fog,

which appears frequently during winter time (mid-October to end of December). Generally, it occurs under stable nighttime conditions (calm wind) and dissipates in early morning as the ground is heated from thermal radiation. In the current study, four sampling sites are chosen from Alsace, which are Geispolsheim (western Strasbourg), Erstein (southwestern Strasbourg), Strasbourg, and Cronenbourg (northwestern Strasbourg) (illustrated in Figure 1), and their characteristics are detailed in Table 1. The sampling sites are close to heavy pollution such as the presence of industrial areas (bordered with Strasbourg), unconventional residential heating (like wood), steel and aluminum factories, agricultural activities (especially in Geispolsheim), and vehicles' exhaust (through the major highway).



**Figure 1.** Map of studied region (Google Earth).

**Table 1.** Characteristics of the four sampling sites.

Characteristic/Site	Geispolsheim	Erstein	Strasbourg	Cronenbourg
Coordinates	48.51469° 7.64373°	48.42273° 7.66326°	48.58461° 7.75071°	48.59449° 7.71621°
Population	7000	11,000	284,677	21,000
City area (Km <sup>2</sup> )	21.9	36.2	78.26	7.03
Landscape topology	Suburban	Rural	Urban	Suburban
Sampler position	4 m AGL	4 m AGL	20 m AGL	4 m AGL

AGL: Above Ground Level.

## 2.2. Fog Collection and Analysis

Fog samples were gathered in glass bottles using the Caltech Active Strand Cloudwater collector (CASCC2) [28,29]. The collector and bottles underwent thorough washing with water and then with ultrapure deionized water (18.2 MΩ cm). Sampling started as the visibility dropped below 300 m. In case the temperature dropped below 0 °C, the collector was immediately turned off to protect the ventilator as well as avoiding the freezing of the collected droplets. Overall, forty-two samples were collected at the four sites during October, November, and December between 2015 and 2021 at the Strasbourg metropolitan area. They were distributed as follows: three samples from Strasbourg in 2016 and 2018; twenty-three samples from Geispolsheim in 2015, 2016, 2017, and 2018; five samples from Cronenbourg in 2018 and 2021; and eleven samples from Erstein in 2015, 2016, and 2018. During 2019 and 2020, there was a complete absence of fog events at the Strasbourg metropolitan area, and thus fog samples could not have been collected in those years. The

majority of radiation fog samples appeared during nighttime conditions (calm wind and clear sky), except a few of them appeared at early morning. Fog events lasted between 2 and 7 h (median of 6 h). Data concerning the collected fog samples are found in Table S1 in the Supplementary Material (SM).

After collection, the sample volume was recorded by weight. The pH and conductivity were directly measured on-site using a pH-meter Consort P407 with a combination micro-electrode (6 mm diameter) Ingold, calibrated against pH 4, 7, and 9 buffers, and a conductivity meter calibrated with standard values of 84 and 1384  $\mu\text{S cm}^{-1}$ , respectively. One milliliter of fog samples was kept for an ion analysis, which was performed directly after collection. Then, fog samples were filtered using a glass microfiber filter with a 0.45  $\mu\text{m}$  porosity. Five to eight milliliters was then acidified with 1% nitric acid ( $\text{HNO}_3$ ) for a heavy metal analysis, which was carried out no later than three days after fog collection. Another five milliliters was used for a dissolved organic carbon (DOC) analysis, while the rest of the solutions were stored in a refrigerator at  $-18\text{ }^\circ\text{C}$  in the dark until analyzing the organic fraction [27,30].

Major cations ( $\text{Ca}^{2+}$ ,  $\text{Mg}^{2+}$ ,  $\text{K}^+$ ,  $\text{Na}^+$ , and  $\text{NH}_4^+$ ) and anions ( $\text{F}^-$ ,  $\text{NO}_2^-$ ,  $\text{SO}_4^{2-}$ ,  $\text{NO}_3^-$ , and  $\text{Cl}^-$ ) were analyzed using the 883 Basic ion chromatography plus (Metrohm, Villebon-sur-Yvette, France) equipped with a high-pressure pump (Ipump), a conductivity detector with a controlled detection stabilizer, and MagIC Net Basic software (version 3.2). A packed bed chemical suppression system was used for anions. For cations, the Metrosep C6 (Metrohm, Villebon-sur-Yvette, France) column (100 mm length, 4 mm internal diameter) was employed with an eluent of 1.7 mM  $\text{HNO}_3$ /1.7 mM PDCA (pyridine-2,6-dicarboxylic acid). For anions, the Metrosep A Supp 4 (Metrohm, Villebon-sur-Yvette, France) column (250 mm length, 4 mm internal diameter) was used with an eluent of 1.8 mM  $\text{Na}_2\text{CO}_3$ /1.7 mM  $\text{NaHCO}_3$ . Both analyses were conducted at a pressure of 7.26 MPa and a flow rate of 1 mL  $\text{min}^{-1}$ .

Major heavy metals (Al, Cr, Mn, Fe, Ni, Cu, Zn, As, Cd, Hg, and Pb) were analyzed using Agilent 7800 Inductively Coupled Plasma-Mass Spectrometry (ICP-MS) (Agilent, Santa Clara, CA, USA) equipped with a High Matrix Introduction (HMI) system and SPS 4 autosampler. The instrument comprises a micromist borosilicate glass concentric nebulizer, a double-pass Peltier-cooled spray chamber, a quartz torch with a 2.5 mm internal diameter, and a high-quality EM detector. The interface components comprised a nickel-plated copper sampling cone and a nickel skimmer cone.

Dissolved organic carbons (DOCs) were determined using a Shimadzu Total Organic Carbon (TOC) analyzer (TOC-5050A) calibrated against potassium hydrogen phthalate standards. The device gives the TOC content in fog samples, which is the sum of the DOC and particles. In our case, fogwater solutions have already been filtered; thus, the DOC is assumed to be equal to the TOC [31]. It has also been proven that DOC constitutes around 80% of TOC in the aqueous phase and concluded that DOC is a nearly quantitative value of TOC in the condensed phase of fogwater [32].

### 2.3. Data Quality

Blank samples were continuously collected by spraying Milli-Q water into the fog collector during the different on-site operation (particularly during cleaning) to evaluate the potential chemical contamination of fog samples. In addition, internal quality control (QC) using reference certified solutions was performed during injections to ensure the absence of impurities. For instance, blanks were used in parallel with the extraction protocol to ensure the absence of the analyzed compounds, blanks of a solvent were also injected between samples to clean the analytical instrument, and control solutions were further injected at the beginning and at the end of each injection series to ensure that the instrument works properly. All blanks were treated as real samples following the same analytical procedures. No significant signs of contamination in the collected water were detected. Some fog samples were measured twice to assess the precision of the analytical procedures.



## 2.4. Statistical Analysis

### 2.4.1. Data Analysis

A Pearson analysis was executed on R (version 4.3.2) correlated with RStudio (version 2023.12.0 + 369). The correlation coefficient matrix is used on the whole data to identify the existing relationship between elements.

### 2.4.2. Non-Sea Salt Fractions

Then, non-sea salt (nss) fractions are calculated to distinguish between sea salt and non-sea salt fractions. The non-sea salt calcium ( $\text{nssCa}^{2+}$ ) is calculated using Equation (1) [33–36].

$$\text{nssCa}^{2+} = \text{Ca}^{2+} - 0.044 * \text{Na}^{+} \quad (1)$$

The non-sea salt sulfate ( $\text{nssSO}_4^{2-}$ ) is calculated using Equation (2).

$$\text{nssSO}_4^{2-} = \text{SO}_4^{2-} - 0.12 * \text{Na}^{+} \quad (2)$$

The average non-sea salt potassium ( $\text{nnsK}^{+}$ ) is calculated using Equation (3).

$$\text{nnsK}^{+} = \text{K}^{+} - 0.022 * \text{Na}^{+} \quad (3)$$

where all concentration units are given in  $\mu\text{Eq L}^{-1}$ .

### 2.4.3. Neutralization and Acidifying Potentials

The neutralization factors (NFs) are computed using Equation (4) to assess the neutralization capacity for the basic components ( $\text{NH}_4^{+}$ ,  $\text{Ca}^{2+}$ , and  $\text{K}^{+}$ ) [37–39].

$$\text{NF}(X) = \frac{[\text{nnsX}^{+}]}{[\text{nssSO}_4^{2-}] + [\text{NO}_3^{-}]} \quad (4)$$

where “X” is the neutralizing cation and  $\text{nnsX}^{+}$  is its non-sea salt equivalent concentration.

The acidifying and neutralizing potential (AP and NP, respectively) are calculated using Equations (5) and (6), respectively [40,41].

$$\text{AP} = \text{nssSO}_4^{2-} + \text{NO}_3^{-} \quad (5)$$

$$\text{NP} = \text{nssCa}^{2+} + \text{NH}_4^{+} \quad (6)$$

### 2.4.4. pAi

To quantify the non-neutralized acidity in fogwater, the quantitative index pAi was introduced [42], which is defined as the negative decimal logarithm of the  $\text{nssSO}_4^{2-}$  concentration plus the  $\text{NO}_3^{-}$  concentration (both ion concentrations are in  $\text{mmol L}^{-1}$ ), as shown in Equation (7). The degree of acid neutralization ( $\Delta\text{pH}$ ) is defined in Equation (8).

$$\text{pAi} = -\log\{[\text{nssSO}_4^{2-}] + [\text{NO}_3^{-}]\} \quad (7)$$

$$\Delta\text{pH} = \text{pH} - \text{pAi} \quad (8)$$

### 2.4.5. Enrichment Factors

The enrichment factors (EFs) of the analyzed heavy metals are computed using aluminum (Al) as the crustal reference using Equation (9) [43]. An EF lower than 10 indicates a non-enriched element (crustal origin), and between 10 and 100 indicates a moderately enriched element, whereas an EF higher than 100 indicates a highly enriched element (mainly from anthropogenic sources).

$$\text{EF} = (\text{X}/\text{Al})_{\text{fog}} / (\text{X}/\text{Al})_{\text{crust}} \quad (9)$$

where  $(X/Al)_{\text{fog}}$  is the individual metal (X) concentration with respect to that of iron in the fog sample, and  $(X/Al)_{\text{crust}}$  is the reference concentration ratio of the metal (X) with respect to iron in the crust. The reference concentrations for Al, Cr, Mn, Ni, Cu, Zn, Hg, As, Cd, and Pb are, respectively, 80,500, 83, 1000, 58, 47, 83, 0.083, 1.7, 0.13, and 16 ppm [44].

#### 2.4.6. Liquid Water Content

The liquid water content (LWC) in fog samples is estimated using Equation (10) [28,45].

$$\text{LWC} = \frac{\text{sample weight(g)}}{\text{sample interval time(min)} * \text{air volume rate}(\text{m}^3\text{min}^{-1}) * 0.8} \quad (10)$$

The constant 0.8 is the estimated collection efficiency for the collector.

### 3. Results and Discussion

#### 3.1. Physico-Chemical Characteristics

Table S2 in the SM summarizes the results of physico-chemical parameters (pH, DOC, LWC, and volume) for individual fog samples.

The median pH values at Geispolsheim, Erstein, Strasbourg, and Cronembourg are, respectively, 6.8, 6.9, 6.7, and 7.4, which are all in accordance with the World Health Organization (WHO) guidelines. There is no remarkable yearly variation during all sampling years, except for a small increase in the pH values from 2016 to 2018 at Geispolsheim, Erstein, and Strasbourg attributed to the decrease in the  $\text{NO}_3^-$  and  $\text{SO}_4^{2-}$  concentrations. The nature of pH has changed over time in the region from acidic to basic. For instance, the average pH range in Strasbourg has increased from 3.5–4 to 6.1–7.4 over the past two decades [21,23] as in other cases in Europe, Asia, and other parts of the world [7,10,46]. Similarly, the ratio of  $[\text{NH}_4^+] / ([\text{SO}_4^{2-}] + [\text{NO}_3^-])$  has increased over time (between 1991 and 2021) mainly due to the substantial decrease in  $\text{SO}_4^{2-}$  and  $\text{NO}_3^-$  concentrations (around 20 times) and the slower decreasing rate of  $\text{NH}_4^+$  levels (around 3 times) (see Figure 2). This is consistent by the observed decrease in the emissions of  $\text{SO}_2$  in Europe and other countries primarily because of the use of fuels containing less sulfur. A similar pH range has been observed in other countries such as Lebanon [30], Bangladesh [47], India [48], and Switzerland [49], and some parts of the US [50], and Poland [41].

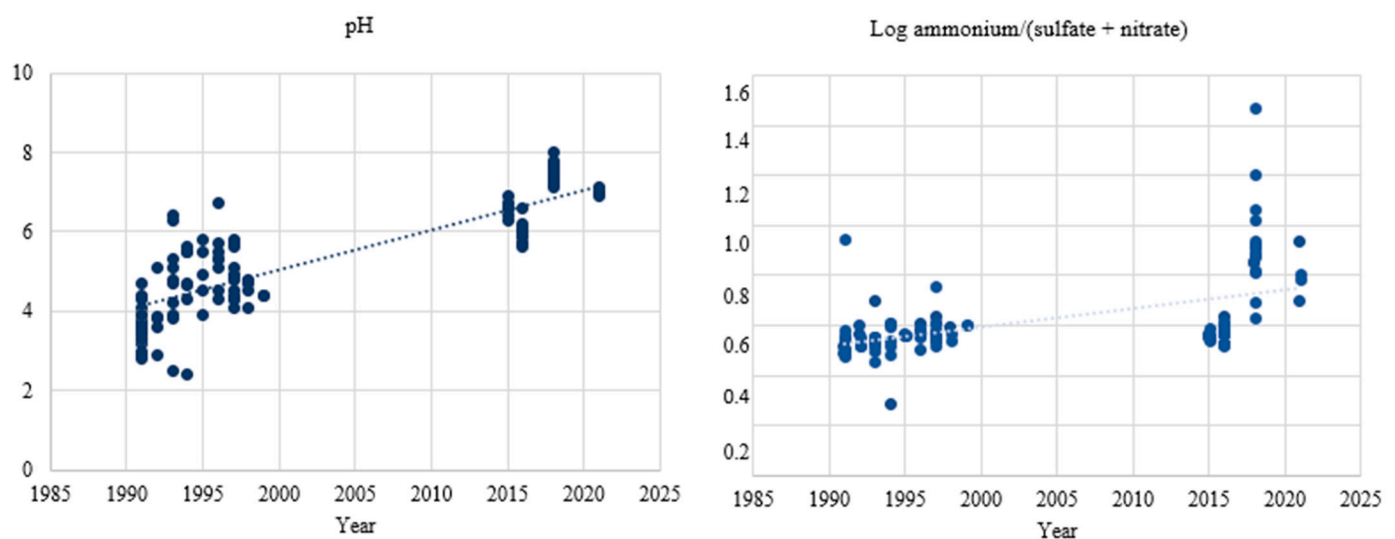


**Figure 2.** The evolution of pH and  $[\text{NH}_4^+] / ([\text{SO}_4^{2-}] + [\text{NO}_3^-])$  in fogwater samples collected at the Strasbourg metropolitan area since 1991 [18]. The lines represent linear regressions.

The median conductivity values at Geispolsheim, Erstein, Strasbourg, and Cronenbourg are, respectively, 110.6, 97.8, 114.4, and 169.8  $\mu\text{S cm}^{-1}$ . The conductivity values fluctuate over time at the first two sites. It has increased from 95.1 to 119.8  $\mu\text{S cm}^{-1}$  and then decreased to 100.1  $\mu\text{S cm}^{-1}$  at Geispolsheim, whereas it has decreased from 131.6 to 109. The reported values vary in the same range with those observed in previous studies such as Kopisty in the Czech Republic (171.9  $\mu\text{S cm}^{-1}$ ) and Baton Rouge in the USA (255  $\mu\text{S cm}^{-1}$ ) [51,52].

DOC levels at Geispolsheim, Erstein, Strasbourg, and Cronenbourg, respectively, vary between 17.4 and 61.5 ppm (median of 24.4 ppm), 20.6 and 35.4 ppm (median of 24.8 ppm), 13.0 and 15.5 ppm (median of 14.3 ppm), and 11.5 and 17.9 ppm (median of 14.7 ppm). There was a decrease in the average DOC levels at Geispolsheim (by 25%) and Erstein (by 30%) between 2015 and 2018, despite the increase between 2016 and 2018 (by 34%). There was also a slight decrease at Strasbourg between 2016 and 2018 by 16%. However, DOC levels at Cronenbourg increased by 40% between 2018 and 2021 mainly due to the impact of the post-COVID-19 pandemic on air pollution [53,54]. The median DOCs at suburban and rural sites are always found to be higher than those at the urban site. The highest DOC levels are obtained at Geispolsheim and Erstein, while Cronenbourg and Strasbourg have almost the same average of DOC levels. The mean DOC levels are lower than those observed in the Po Valley (62 ppm), but much higher than Delta Barrage (9.7 ppm), Houston (11.5 ppm), Mt. Eden (9 ppm), and Baton Rouge (6 ppm) [52,55,56]. Additionally, the DOCs at Cronenbourg and Strasbourg are also lower than those reported in Bakersfield (27 ppm) and Fresno (20 ppm). In contrast, the DOC levels at Geispolsheim and Erstein vary in the same order of magnitude as those found in Bakersfield and Fresno [57].

The median LWC values vary almost in the same range at all sites. It is the lowest at Strasbourg (37.8  $\text{g m}^{-3}$ ), followed by Cronenbourg (51.0  $\text{g m}^{-3}$ ), Geispolsheim (59.7  $\text{g m}^{-3}$ ), and Erstein (69.5  $\text{g m}^{-3}$ ). The LWC is relatively low to collect important fog volume. For instance, the median fog volumes at the four sampling sites vary between 40 and 95 mL. The median LWC is higher than that calculated in 1996 (median of 20  $\text{g m}^{-3}$ ) where larger fog volumes were collected [23].

### 3.2. Ion Analysis

#### 3.2.1. Quality Control

The cation–anion balance is used to assess data reliability before the analysis. The mean ratios of the sum of cations to that of anions are close to unity during 2015, 2016, and 2017, varying between 0.8 and 1.5 at all sampling sites (see Figure 3). However, there is an apparent anion deficiency (cation excess) in fogwater samples collected during 2018 and 2021 at all sites. The first significant reason could be attributed to the substantial decrease in  $\text{NO}_3^-$  and  $\text{SO}_4^{2-}$  concentrations, with a continuous increase in  $\text{NH}_4^+$  levels. Their decrease is mainly due to the use of catalytic filters and converters for vehicles working on diesel or fuel oil, the use of less sulfur-containing fossil fuels (coal and fuel oil), improvements in the energy efficiency of industrial installations, and some possible changes in redox conditions in the atmosphere. Further, ion deficiency might come from not measuring enough anions (soluble organic compounds such as formate and acetate) compared to cations. Given that ion balance is not performed, samples gathered during 2018 and 2021 are not compared with previous ones. Instead, the evolution of annual element flows is preferred in the current study. The conductivity balance (measured vs. theoretical) is also acceptable ( $R^2 = 0.81$ ) for the same sampling years, but not totally perfect due to the instrumental uncertainty [58–63].

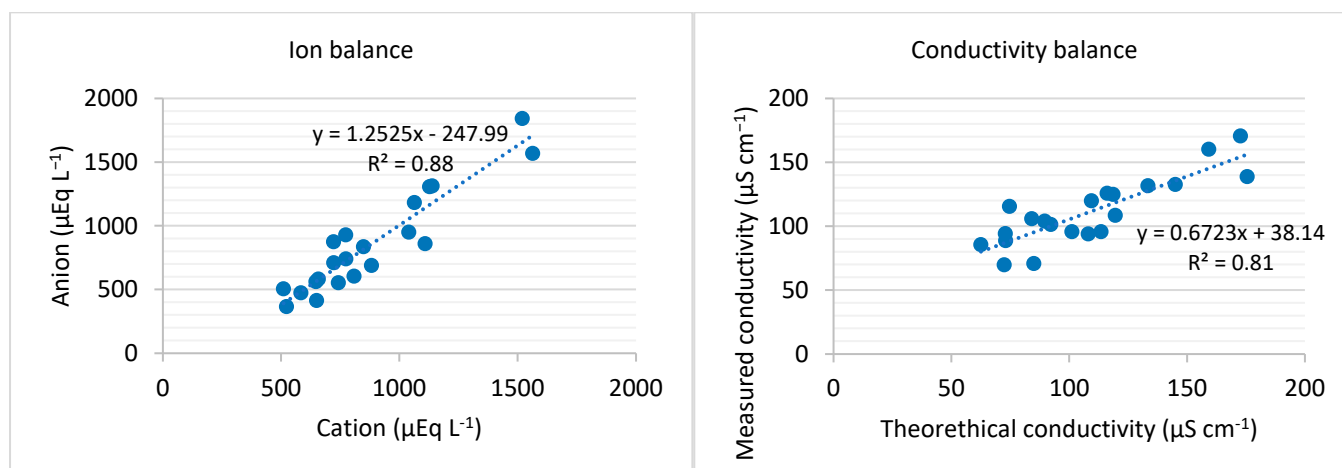


**Figure 3.** Ion and conductivity balance for samples taken during 2015, 2016, and 2017.

### 3.2.2. Ionic Concentration

Table S3 in the SM shows the analysis results of the investigated ions for each fog sample. The highest mean TIC is obtained at Strasbourg (STG) (mean of  $1952.4 \mu\text{Eq L}^{-1}$ ), followed by Cronenbourg (CR) (mean of  $1923.6 \mu\text{Eq L}^{-1}$ ), followed by Geispolsheim (G) (mean of  $1493.7 \mu\text{Eq L}^{-1}$ ), and Erstein (ER) (mean of  $1338.3 \mu\text{Eq L}^{-1}$ ). A good correlation is found between TIC and K ( $p < 0.05$ ), indicating that a higher conductivity value corresponds to a higher concentration in the fog sample. Additionally, the analysis shows the effect of the collected volume on fog solute concentration, which are inversely proportional. This means that an increase in fog volume tends to dilute the sample [24]. LWC is an important factor that controls fog chemistry and has been previously investigated in many research papers [5,7,30,34,43,64,65]. The graph shows an inverse relationship between LWC and fog solute concentration, regardless of the sampling location. An increase in liquid content causes a dilution of the solute in fog samples (decreases its concentration).

In the current study, the ionic strength at Strasbourg is much lower than that reported previously in the same region. The concentrations of all ions have decreased compared to the historical values measured at the same site [21,23]. The average concentrations of individual ions obtained in the current study are compared with those obtained in a pristine environment (Borucino, Poland) and a polluted city (Shanghai, China), and the results show that they are even lower than the pristine location [2,41].

### 3.2.3. Annual Element Chart

Figure 4 shows the evolution of annual median element concentrations ( $\mu\text{Eq L}^{-1}$ ) at the four sampling locations over the sampling period. The graph shows either a decrease or an increase in the individual element levels over time. Wet deposition can be one of the main reasons for the yearly trend in the TIC. It is also well known that temporal evolution of air pollutant loadings is very correlated with weather conditions (wind, relative humidity, and temperature), which lead either to their dispersion or accumulation in the ambient atmosphere. Differences in emissions could also be another factor responsible for the decrease/increase in the TIC [34,66].



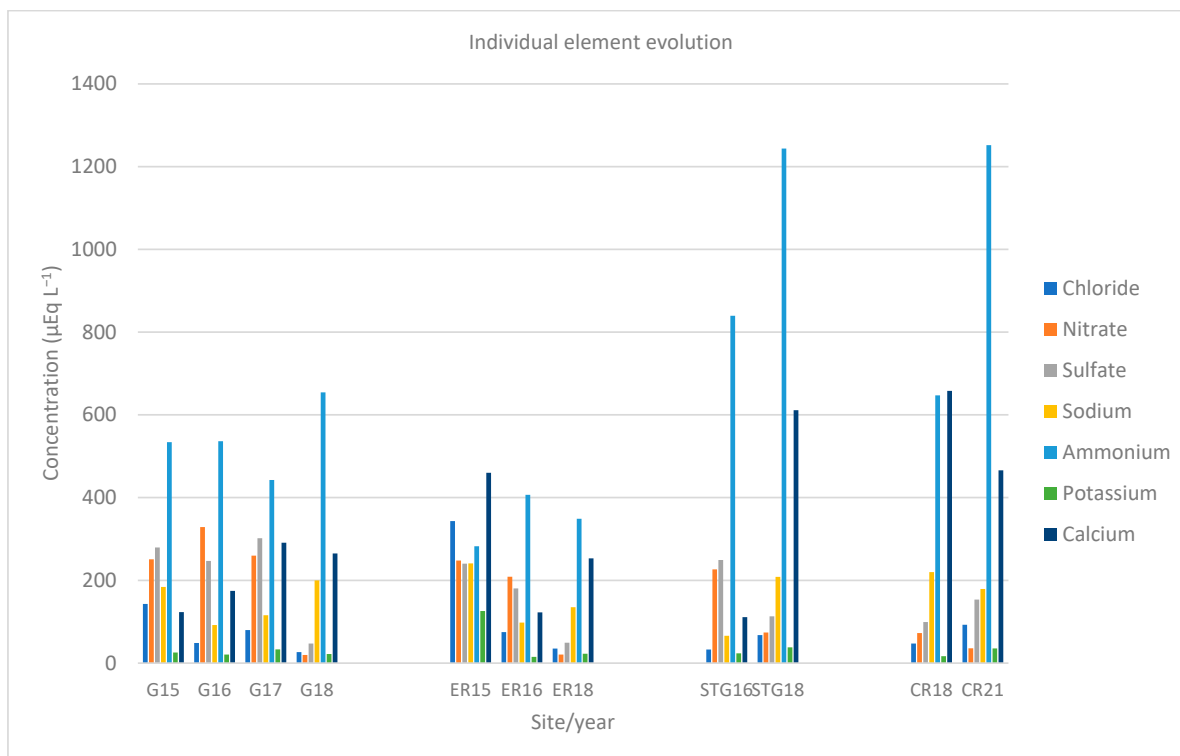


**Figure 4.** Median ion concentration evolutions ( $\mu\text{Eq L}^{-1}$ ) at the four sites. G: Geispolsheim; ER: Erstein; STG: Strasbourg; CR: Cronenbourg.

The dominant cation species observed for all fog events are  $\text{NH}_4^+$  and  $\text{Ca}^{2+}$ , accounting for a mean of 60% of the TIC, while the dominant anion species are  $\text{NO}_3^-$  and  $\text{SO}_4^{2-}$ , accounting for a mean of 22% of the TIC.

In our study,  $\text{Ca}^{2+}$  mainly results from the mineral dust released from cement released during different construction activities and land erosion (such as renovation of Strasbourg University, construction of new buildings, etc.) [2]. Its concentration levels vary from 3.5 to 1996.0  $\mu\text{Eq L}^{-1}$  (median of 192.3  $\mu\text{Eq L}^{-1}$ ), and it is detected in all fog samples. The median level of  $\text{Ca}^{2+}$  has increased over time at Geispolsheim and Strasbourg, whereas it has decreased at Erstein and Cronenbourg. To separate between  $\text{Ca}^{2+}$  originating from sea salt and non-sea salt, the  $\text{nssCa}^{2+}$  fraction is calculated for each fog sample. The results show that the median ratios of  $\text{nssCa}^{2+}$  to the total  $\text{Ca}^{2+}$  fraction at all sites are higher than 92% (see Table S4 in the SM). This indicates that the contribution of  $\text{Ca}^{2+}$  from sea salts is negligible, since all sites are far from seas and oceans.  $\text{Ca}^{2+}$  can be further emitted from the soil nature at Strasbourg and its vicinity composed of loess (very rich in  $\text{Ca}^{2+}$ ), comprising fine dust particles that are easily spread by air currents [23].

The presence of  $\text{NH}_4^+$  is directly linked to the input of ammonia ( $\text{NH}_3$ ) into fog droplets, especially those coming from agricultural activities, fertilizer industries, decomposition of animal wastes, and biomass burning, and indirectly due to the input coming from  $\text{NH}_3$  aerosols [67]. In addition to these factors, it can severely result from road traffic, which is linked to the use of catalytic converters in vehicles [68]. There is a significant emission of  $\text{NH}_3$  in our sampling site since all sites are either affected by the presence of farms or situated in proximity to the main highway. The median levels of  $\text{NH}_4^+$  have become more important over time at Geispolsheim (increase from 533.9 to 667.8  $\mu\text{Eq L}^{-1}$ ), Erstein (increase from 282.2 to 348.9  $\mu\text{Eq L}^{-1}$ ), Strasbourg (increase from 839.4 to 1243.6  $\mu\text{Eq L}^{-1}$ ), and Cronenbourg (increase from 647.2 to 1251.7  $\mu\text{Eq L}^{-1}$ ). The increase in its amount over the sampling years might be linked to weather conditions (such as the increase in skin temperature) that lead to the volatilization of applied mineral fertilizers in the sampled sites into the atmosphere and their scavenging by fog. Soil characteristics can also play a

major role for the volatilization of ammonium. For instance, a basic soil pH in a dry climate favors the emission of ammonia into the air, thus increasing its levels. Additionally, the introduction of the selective catalytic reduction (SCR) system in vehicles can lead to the increase in ammonia emissions associated with road traffic [68]. The high levels at the urban site Strasbourg also further suggest the probable effect of LRT on pollutant loadings from rural sites to nearby regions. However, further records are needed to confirm these conclusions.

The presence of  $\text{NO}_3^-$  is frequently related to the direct input of gaseous  $\text{HNO}_3$ , which is released from vehicular exhaust, as well as to the indirect input resulting from  $\text{NO}_3^-$  aerosol scavenging.  $\text{SO}_4^{2-}$  is mainly derived either from  $\text{SO}_4^{2-}$  aerosol scavenging or the in situ oxidation of its precursor gas, sulfur dioxide ( $\text{SO}_2$ ), released from the combustion of fossil fuels (such as lignite) [69,70]. Thus, the presence of  $\text{NO}_3^-$  and  $\text{SO}_4^{2-}$  could be mainly attributed to the large consumption of coal in Alsace where coal burning is the primary energy source used in this region, especially in rural and suburban sites [71,72]. They can be further released from some steel and aluminum factories that are located in the industrial city “Kehl”, whose emissions can be transported by winds to other nearby locations. A sharp decrease for both ions is observed for all sites over the sampling, except for a small increase at Cronenbourg between 2018 and 2021 from 99.1 to 153.3  $\mu\text{Eq L}^{-1}$ .  $\text{SO}_4^{2-}$  may have further emissions attributed to sea salts (marine contributions). For instance, the individual ratios of  $\text{SO}_4^{2-}$  to  $\text{Na}^+$  are all higher than that of sea water (0.12) (median of 0.9), implying that  $\text{SO}_4^{2-}$  does not originate from sea salt particles, and the marine contributions are, therefore, very weak or negligible (see Table S4 in the SM). This means that Alsace is more influenced by local sources rather than the LRT of pollutants. The calculated median  $\text{nssSO}_4^{2-}$  fraction is 88%, proving the non-significance of the sea salt effect. Additionally, the ratio of  $\text{NO}_3^-$  to  $\text{SO}_4^{2-}$  is widely employed to predict the relative significance of nitrogen oxide ( $\text{NO}_x$ ) (vehicles) versus stationary  $\text{SO}_2$  (power plants). In this study, the individual ratios of  $\text{NO}_3^-$  to  $\text{SO}_4^{2-}$  vary from 0.1 to 2.3 (median of 0.7), indicating that the contribution of  $\text{SO}_4^{2-}$  is more important than  $\text{NO}_3^-$  for the majority of cases (see Figure 5). In some cases,  $\text{NO}_3^-/\text{SO}_4^{2-}$  reaches values as low as 0.1, indicating that  $\text{SO}_4^{2-}$  originates from a single origin rather than different ones [73]. For some events, the ratio is higher than unity (even bigger than two for one fog event at Geispolsheim), implying that  $\text{NO}_3^-$  levels are higher than those of  $\text{SO}_4^{2-}$ . The median  $\text{NO}_3^-/\text{SO}_4^{2-}$  has decreased over the sampling period at all sites, proving that the concentrations of  $\text{SO}_4^{2-}$  have gradually decreased (see Table S4 in the SM).

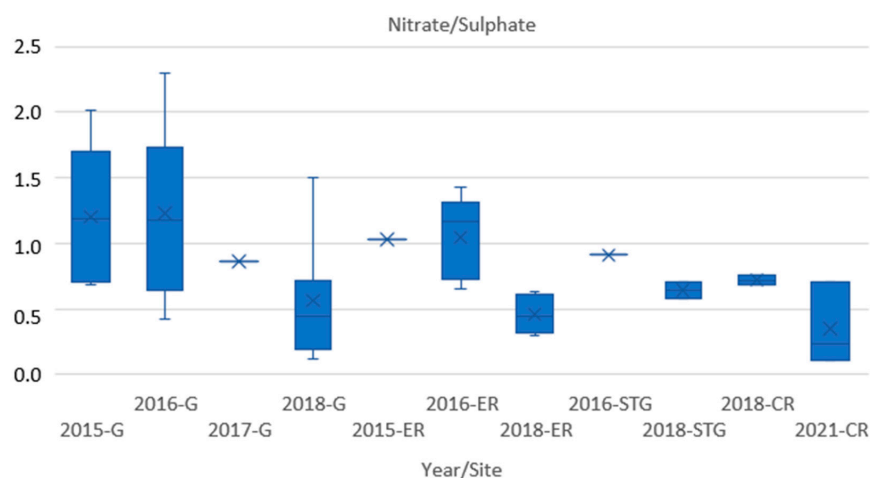


**Figure 5.** A boxplot of the nitrate-to-sulfate ratio at all sites and years. G: Geispolsheim; ER: Erstein; STG: Strasbourg; CR: Cronenbourg.

$\text{Cl}^-$  is generally derived from droplet scavenging of sea salt particularly in regions impacted by oceanic air masses. Its median levels have decreased over time at Geispolsheim (from 142.9 to 26.5  $\mu\text{Eq L}^{-1}$ ) and Erstein (from 343.2 to 35.2  $\mu\text{Eq L}^{-1}$ ), whereas they have increased at Strasbourg (from 32.9 to 67.6  $\mu\text{Eq L}^{-1}$ ) and Cronenbourg (from 47.2 to 92.6  $\mu\text{Eq L}^{-1}$ ). In the current study, the calculated ratio of  $\text{Cl}^-/\text{Na}^+$  is quite different than that of sea water (1.17). For instance, the median ratios of  $\text{Cl}^-/\text{Na}^+$  are different than 1.17, indicating its anthropogenic origin (see Table S4 in the SM). In addition to sea salts,  $\text{Cl}^-$  might be derived from fossil fuel combustion, waste incineration, and vehicular emissions since gasoline contains lead bromo-chloride as an additive [23,74]. However, the leaded gasoline is banned in Europe; thus,  $\text{Cl}^-$  emission released from leaded gasoline is not significant in the region under study. One of the most probable emission sources for  $\text{Cl}^-$  is the incinerator that is almost 4 km away from Strasbourg. Other sampling sites might also be affected since the discharges are emitted in all directions around the incinerator [23].  $\text{Cl}^-$  can be further released from paper industries, which use chloride in the vapor phase, but such factories are not present near our sampling sites.  $\text{Na}^+$  can be derived from soil dust and biomass combustion used for cooking as well as droplet scavenging from sea water. Its median levels have decreased over time at Erstein (from 240.9 to 135.2  $\mu\text{Eq L}^{-1}$ ) and Cronenbourg (from 220.0 to 179.1  $\mu\text{Eq L}^{-1}$ ), whereas they have increased at Geispolsheim (from 183.9 to 200.1  $\mu\text{Eq L}^{-1}$ ) and Strasbourg (from 66.1 to 208.5  $\mu\text{Eq L}^{-1}$ ).

$\text{Mg}^{2+}$ , which most frequently originates from sea salt droplet scavenging as well as re-suspended road dust and LRT of dust transport, is only quantified in fog samples collected in 2018 and 2021 at Strasbourg and Cronenbourg.  $\text{K}^+$  is mainly emitted from biomass burning as well as sea salt scavenging [2]. For instance, the median  $\text{nnsK}^+$  is 87 %, indicating the minor marine contribution in the studied region (primarily from the North Atlantic Ocean) (see Table S4 in the SM). On one hand, the median levels of  $\text{K}^+$  have largely decreased at Erstein from 125.9 to 22.6  $\mu\text{Eq L}^{-1}$ , whereas a small increase has been detected at Geispolsheim (from 25.7 to 21.8  $\mu\text{Eq L}^{-1}$ ). On the other hand, an increase in the  $\text{K}^+$  levels has been observed at Strasbourg (from 23.6 to 38.2  $\mu\text{Eq L}^{-1}$ ) and Cronenbourg (from 16.6 to 35.5  $\mu\text{Eq L}^{-1}$ ).

#### 3.2.4. Neutralization and Acidifying Potentials

The calculated NFs for  $\text{Ca}^{2+}$ ,  $\text{K}^+$ , and  $\text{NH}_4^+$  along with AP, NP, and AP/NP are shown in Table S4 in the SM. The highest NFs are obtained in 2018, where  $\text{SO}_4^{2-}$  and  $\text{NO}_3^-$  levels are the lowest. The same order of neutralization is observed at all sites over all sampling years,  $\text{NH}_4^+$ ,  $\text{Ca}^{2+}$ , and  $\text{K}^+$ . The results further show that NP values are higher than AP values, proving the effect of alkaline components toward the neutralization of the acidic species.  $\text{NH}_4^+$  concentrations, in nine samples, are lower than their corresponding AP values, showing that  $\text{NH}_4^+$  is not capable alone to neutralize the acidity. The rest of the samples have an excess of  $\text{NH}_4^+$  compared with AP, which is responsible for the high pH values. Thus, fogwater neutralization is mainly caused either by both coarse particles or  $\text{NH}_3$  scavenging. If the latter is the main process,  $\text{NH}_4^+$  would be in excess. However, if the former process dominates, then  $\text{NH}_4^+$  would be less than AP. In case  $\text{NH}_4^+$  is in excess, it might also neutralize other anions such as organic acids [34].

#### 3.2.5. pAi and pH

The calculated values of pAi vary between 6.0 and 8.0, and the differences between pH and pAi vary between 0.01 and 0.9 (see Figure 6 and Table S4 in the SM). The negligible difference (0.01) between pAi and pH indicates the negligible neutralizing effect and that acidic components are merely neutralized. The large difference (0.9) between both values indicates that fogwater would be much more acidic if there would not have been a strong neutralization effect.

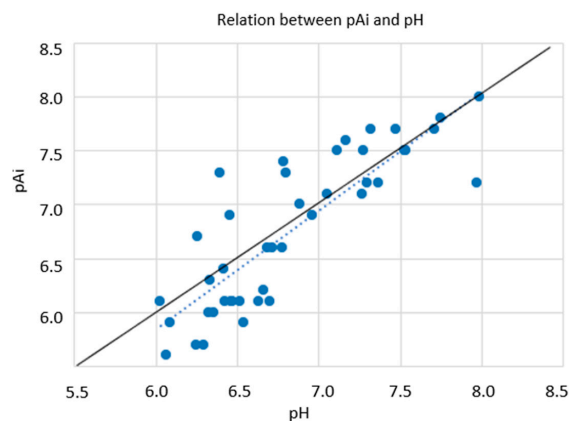


**Figure 6.** Relation between pAi and pH for all fog samples. The dotted line represents the linear regression line.

### 3.3. Heavy Metals

#### 3.3.1. Element Concentration

Table S5 in the SM shows the analysis result of heavy metals in fog samples. The analysis shows that the highest median concentration is observed at Cronenbourg ( $2860.3 \mu\text{g L}^{-1}$ ), followed by Geispolsheim and Strasbourg ( $1846.4 \mu\text{g L}^{-1}$  and  $1819.7 \mu\text{g L}^{-1}$ , respectively), and Erstein ( $1547.2 \mu\text{g L}^{-1}$ ).

#### 3.3.2. Sources of Heavy Metals

Figure 7 shows the individual median concentration ( $\mu\text{g L}^{-1}$ ) of the dominant heavy metals over the sampling years at the four sites. Al, Mn, Fe, Ni, Cu, and Zn are the majority in fog samples, whereas the rest (As, Cd, Cr, Pb, and Hg) are detected at very low levels ranging from  $0.6$  to  $7.7 \mu\text{g L}^{-1}$ , accounting for less than 0.6%. The two most abundant elements at all sites are Zn and Ni, accounting together for more than 78%, and their median concentration levels vary, respectively, in the range of  $744.9$ – $2161.7 \mu\text{g L}^{-1}$  and  $165.0$ – $666.6 \mu\text{g L}^{-1}$ . Other metals such as Al, Mn, and Fe account together for less than 10% of the total elemental fraction, and their concentration ranges vary, respectively, in the range of  $23.2$ – $77.5 \mu\text{g L}^{-1}$ ,  $29.7$ – $189.6 \mu\text{g L}^{-1}$ , and  $24.4$ – $72.7 \mu\text{g L}^{-1}$ . The decreasing order of the five least abundant metals detected in fogwater is Hg, Cr, Pb, Cd, and As, whose median levels vary from  $0.4$  to  $8.4 \mu\text{g L}^{-1}$ . Those five heavy metals are known for their high toxicity to human health and the environment, and fortunately their levels in fog samples are very low in most cases.

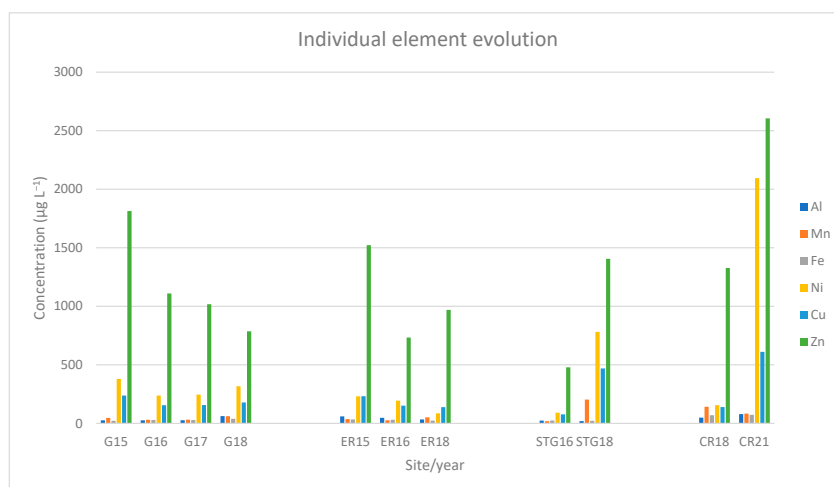


**Figure 7.** Individual median metal concentration ( $\mu\text{g L}^{-1}$ ) over the sampling years at the four sites. G: Geispolsheim; ER: Erstein; STG: Strasbourg; CR: Cronenbourg.

The median EFs for the analyzed elements at all sites are summarized in Table 2. In the current study, the median EF values for Cr, Mn, Fe, As, and Pb are much lower than 10, indicating their crustal origin (non-enriched elements). Crustal sources are attributed to the presence of Fe, small suspended particles of soil, and vehicle motors made from Al are associated with the presence of the latter, and the incineration of products containing Mn is linked to the atmospheric presence of the latter. The very low Pb concentrations in Alsace can be explained by the shift to the use of unleaded fuels in France and surrounding regions since 1989 [23]. Zn, Cd, and Hg have median EF values between 10 and 100 (moderately enriched), indicating the moderate influence of anthropogenic origins for these elements. Zn usually exists at low levels in soils; thus, most of it comes mainly from anthropogenic activities including the steel and aluminum industries. That is why Strasbourg and Cronenbourg are highly contaminated by Zn, whose median levels are, respectively, 1326.3 and 2161.7  $\mu\text{g L}^{-1}$ . Ni and Cu are more enriched at Strasbourg and Cronenbourg (EF between 10 and 100) than Geispolsheim and Erstein (EF between 1 and 10). The reasons attributed to the high Ni levels could be the incineration, fuel combustion, and metal production factories, which are also more important at Strasbourg and Cronenbourg (666.6 and 350.0  $\mu\text{g L}^{-1}$ , respectively). Cu, which is primarily derived from vehicle brake pad wear and metal production (according to the National Atmospheric Emission Inventory), comes third with median concentration levels varying in the range of 151.9–418.5  $\mu\text{g L}^{-1}$ . Its levels are the highest at the urban site Strasbourg (418.5  $\mu\text{g L}^{-1}$ ) and the lowest at the rural site Erstein (151.9  $\mu\text{g L}^{-1}$ ).

**Table 2.** Average EF values for the analyzed elements at the four locations.

	Cr	Mn	Fe	Ni	Cu	Zn	Cd	Hg	As	Pb
Geispolsheim	0.047	0.096	0.002	9.7	9.5	31.2	30.2	86.2	0.7	0.3
Erstein	0.043	0.071	0.001	4.6	5.8	18.9	12.0	48.4	0.5	0.2
Strasbourg	0.118	0.753	0.002	53.7	30.9	62.1	67.4	269.5	2.3	0.3
Cronenbourg	0.071	0.215	0.002	11.9	12.3	27.1	24.3	54.1	0.7	0.2

In the current study, the concentration levels found vary within the same range as those observed in Riverside (California) [75], New Delhi (India) [76], and Po Valley (Italy) [77], but are lower than those observed in Baton Rouge (Louisiana) [50], Milesovka (Czech) [78], Delta Barrage (Egypt) [56], and Coastal Island (Bangladesh) [47]. The concentrations of Cu, Pb, Fe, Zn, and Mn found in this study are much lower than those found in the most recent fog studies in Delta Barrage (Egypt) [56], Coastal Island (Bangladesh) [47], and Milesovka (Czech) [78]. Additionally, the total and individual concentration levels of the investigated heavy metals reported in the current study are much lower than those found previously in 1996 at Strasbourg [23].

### 3.4. Statistical Analyses

#### Pearson Correlation

Pearson correlation coefficients for fogwater quality data are shown in Figure 8. The correlation analysis shows a reasonable significant relationship among different chemical parameters such as  $\text{Cl}^-$  and  $\text{Na}^+$ ,  $\text{SO}_4^{2-}$  and  $\text{NO}_3^-$ , and heavy metals and  $\text{Na}^+$ . The good correlation (0.78,  $p < 0.001$ ) observed between  $\text{Cl}^-$  and  $\text{Na}^+$  proves that  $\text{Cl}^-$  is derived from anthropogenic activities. The good correlation between  $\text{SO}_4^{2-}$  and  $\text{NO}_3^-$  (0.83,  $p < 0.001$ ) suggests that both originate mainly from anthropogenic sources (such as vehicular transport and industries). There are correlations that are observed between  $\text{NH}_4^+$  and  $\text{NO}_3^-$  and between  $\text{NH}_4^+$  and  $\text{SO}_4^{2-}$ , which indicates the un-existence of atmospheric  $(\text{NH}_4)_2\text{SO}_4$ ,  $\text{NH}_4\text{HSO}_4$ , and  $\text{NH}_4\text{NO}_3$  aerosols (in contrast with [36]). The weak correlations between  $\text{Na}^+$  and both  $\text{Ca}^{2+}$  and  $\text{SO}_4^{2-}$  proves the absence of sea droplet scavenging. The strong inter-correlations ( $p < 0.001$ ) among the analyzed heavy metals show that they share the same pollution source. Weak correlations have been found between heavy metals with



$\text{NH}_4^+$  and  $\text{K}^+$ , whereas that found with  $\text{Na}^+$  is stronger ( $p < 0.001$ ), indicating the modest marine influence.

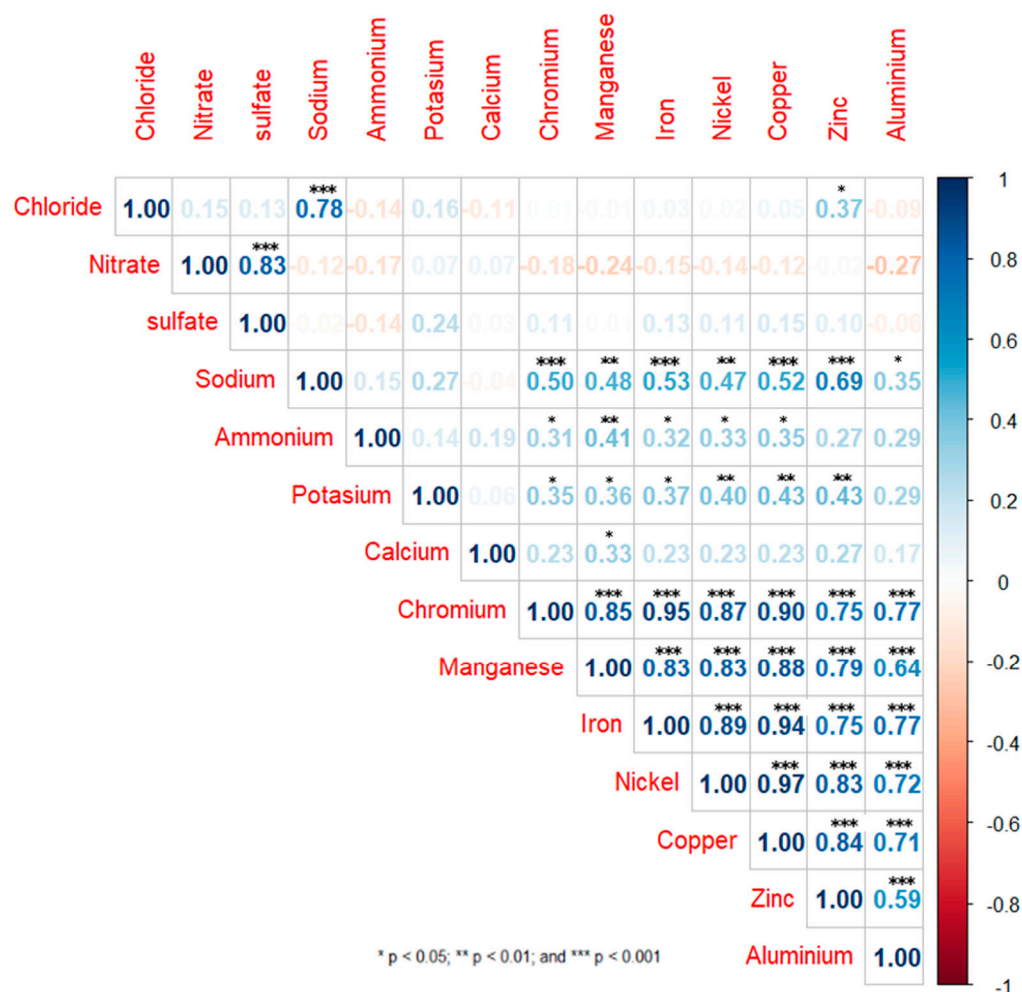


Figure 8. Pearson correlation coefficients for fogwater quality data.

#### 4. Conclusions

A comprehensive fog experiment in the Alsace region was successfully conducted between 2015 and 2021 at four sites, Strasbourg, Geispolsheim, Erstein, and Cronenbourg, aimed to assess the spatio-temporal evolution of the chemical composition and physico-chemical properties. For this purpose, a total of forty-two radiation fog samples were collected and analyzed for their major inorganic ions, heavy metals, and physico-chemical properties. The investigations showed that the pH nature has changed over time from acidic (1990s) to basic. This was found to be correlated with the rapid decrease in nitrate ( $\text{NO}_3^-$ ) and sulfate ( $\text{SO}_4^{2-}$ ) levels (around 20 times). The main ions found at all sites are  $\text{NH}_4^+$ ,  $\text{Ca}^{2+}$ ,  $\text{NO}_3^-$ , and  $\text{SO}_4^{2-}$ , accounting for more than 80% of total ionic concentration (TIC). The marine contribution to  $\text{SO}_4^{2-}$ ,  $\text{Ca}^{2+}$ , and  $\text{K}^+$  is found to be negligible in the investigated region, due to its far location from the sea and ocean. The two dominant elements found at all sites are Zn and Ni, which account together for more than 78% of the total elemental fraction. Local anthropogenic emissions are suggested to be the main source of pollution in Alsace rather than the long-range transport (LRT). The anthropogenic sources responsible for fog contamination include vehicle exhaust, industries, agriculture, and biomass burning. To conclude, it is highly recommended to continuously monitor fog chemistry as a valuable means to check the effectiveness of current policies and try to further update air strategies to enhance air quality in the studied region.

**Supplementary Materials:** The following supporting information can be downloaded at: <https://www.mdpi.com/article/10.3390/air2030014/s1>, Table S1: Samples collected from the Alsace region at the four sampling sites during all years; Table S2: Physico-chemical properties of fog samples; Table S3: Anion and cation analysis results in fog samples; Table S4: Statistical analysis for fog samples; Table S5: Analysis results for heavy metals in fog samples.

**Author Contributions:** Conceptualization, D.K., M.M., Y.J. and O.D.; methodology and experimentation: D.K. and T.W.; validation, D.K., M.M., Y.J. and O.D.; data curation, D.K.; writing—original draft preparation, D.K.; review and editing, D.K., M.M., Y.J., T.W. and O.D.; supervision, M.M., Y.J. and O.D.; project administration, M.M. All authors have read and agreed to the published version of the manuscript.

**Funding:** This research received no external funding.

**Institutional Review Board Statement:** Not applicable.

**Informed Consent Statement:** Not applicable.

**Data Availability Statement:** Data in this study are available upon request.

**Conflicts of Interest:** The authors declare no conflicts of interest.

## References

1. Yang, J.; Xie, Y.-J.; Shi, C.-E.; Liu, D.-Y.; Niu, S.-J.; Li, Z.-H. Ion Composition of Fog Water and Its Relation to Air Pollutants during Winter Fog Events in Nanjing, China. *Pure Appl. Geophys.* **2012**, *169*, 1037–1052. [[CrossRef](#)]
2. Li, P.; Li, X.; Yang, C.; Wang, X.; Chen, J.; Collett, J.L., Jr. Fog water chemistry in Shanghai. *Atmos. Environ.* **2011**, *45*, 4034–4041. [[CrossRef](#)]
3. Mohan, M.; Payra, S. Influence of Aerosol Spectrum and Air Pollutants on Fog Formation in Urban Environment of Megacity Delhi, India. *Environ. Monit. Assess.* **2009**, *151*, 265–277. [[CrossRef](#)] [[PubMed](#)]
4. Gultepe, I.; Tardif, R.; Michaelides, S.C.; Cermak, J.; Bott, A.; Bendix, J.; Müller, M.D.; Pagowski, M.; Hansen, B.; Ellrod, G.; et al. Research: A Review of Past Achievements and Future Perspectives. *Pure Appl. Geophys.* **2007**, *164*, 1121–1159. [[CrossRef](#)]
5. Elbert, W. Control of Solute Concentrations in Cloud and Fog Water by Liquid Water Content. *Atmos. Environ.* **2000**, *34*, 1109–1122. [[CrossRef](#)]
6. Herckes, P.; Valsaraj, K.T.; Collett, J.L. A Review of Observations of Organic Matter in Fogs and Clouds: Origin, Processing and Fate. *Atmos. Res.* **2013**, *132–133*, 434–449. [[CrossRef](#)]
7. Giulianelli, L.; Gilardoni, S.; Tarozzi, L.; Rinaldi, M.; Decesari, S.; Carbone, C.; Facchini, M.C.; Fuzzi, S. Fog Occurrence and Chemical Composition in the Po Valley over the Last Twenty Years. *Atmos. Environ.* **2014**, *98*, 394–401. [[CrossRef](#)]
8. van Pinxteren, D.; Fomba, K.W.; Mertes, S.; Müller, K.; Spindler, G.; Schneider, J.; Lee, T.; Collett, J.L.; Herrmann, H. Cloud Water Composition during HCCT-2010: Scavenging Efficiencies, Solute Concentrations, and Droplet Size Dependence of Inorganic Ions and Dissolved Organic Carbon. *Atmos. Chem. Phys.* **2016**, *16*, 3185–3205. [[CrossRef](#)]
9. Seinfeld, J.H.; Pandis, S.N. From air pollution to climate change. In *Atmospheric Chemistry and Physics*; John Wiley & Sons, Inc.: Hoboken, NJ, USA, 1998; Volume 1326.
10. Li, H.; Wu, H.; Wang, Q.; Yang, M.; Li, F.; Sun, Y.; Qian, X.; Wang, J.; Wang, C. Chemical Partitioning of Fine Particle-Bound Metals on Haze–Fog and Non-Haze–Fog Days in Nanjing, China and Its Contribution to Human Health Risks. *Atmos. Res.* **2017**, *183*, 142–150. [[CrossRef](#)]
11. Kim, H.; Collier, S.; Ge, X.; Xu, J.; Sun, Y.; Jiang, W.; Wang, Y.; Herckes, P.; Zhang, Q. Chemical Processing of Water-Soluble Species and Formation of Secondary Organic Aerosol in Fogs. *Atmos. Environ.* **2019**, *200*, 158–166. [[CrossRef](#)]
12. Izhar, S.; Gupta, T.; Panday, A.K. Scavenging Efficiency of Water-Soluble Inorganic and Organic Aerosols by Fog Droplets in the Indo Gangetic Plain. *Atmos. Res.* **2020**, *235*, 104767. [[CrossRef](#)]
13. Goodman, J. The Microstructure of California Coastal Fog and Stratus. *J. Appl. Meteor.* **1977**, *16*, 1056–1067. [[CrossRef](#)]
14. Zannetti, P.; Melli, P.; Runca, E. Meteorological Factors Affecting SO<sub>2</sub> Pollution Levels in Venice. *Atmos. Environ.* **1977**, *11*, 605–616. [[CrossRef](#)] [[PubMed](#)]
15. Watanabe, K.; Honoki, H.; Iwai, A.; Tomatsu, A.; Noritake, K.; Miyashita, N.; Yamada, K.; Yamada, H.; Kawamura, H.; Aoki, K. Chemical Characteristics of Fog Water at Mt. Tateyama, Near the Coast of the Japan Sea in Central Japan. *Water Air Soil. Pollut.* **2010**, *211*, 379–393. [[CrossRef](#)]
16. Yue, Y.; Niu, S.; Zhao, L.; Zhang, Y.; Xu, F. Chemical Composition of Sea Fog Water Along the South China Sea. *Pure Appl. Geophys.* **2012**, *169*, 2231–2249. [[CrossRef](#)]
17. Vautard, R.; Yiou, P.; van Oldenborgh, G.J. Decline of Fog, Mist and Haze in Europe over the Past 30 Years. *Nat. Geosci.* **2009**, *2*, 115–119. [[CrossRef](#)]
18. Quan, J.; Zhang, Q.; He, H.; Liu, J.; Huang, M.; Jin, H. Analysis of the Formation of Fog and Haze in North China Plain (NCP). *Atmos. Chem. Phys.* **2011**, *11*, 8205–8214. [[CrossRef](#)]

19. Fu, G.Q.; Xu, W.Y.; Yang, R.F.; Li, J.B.; Zhao, C.S. The Distribution and Trends of Fog and Haze in the North China Plain over the Past 30 Years. *Atmos. Chem. Phys.* **2014**, *14*, 11949–11958. [[CrossRef](#)]
20. Herckes, P.; Marcotte, A.R.; Wang, Y.; Collett, J.L. Fog Composition in the Central Valley of California over Three Decades. *Atmos. Res.* **2015**, *151*, 20–30. [[CrossRef](#)]
21. Herckes, P.; Wortham, H.; Mirabel, P.; Millet, M. Evolution of the Fogwater Composition in Strasbourg (France) from 1990 to 1999. *Atmos. Res.* **2002**, *64*, 53–62. [[CrossRef](#)]
22. Millet, M.; Wortham, H.; Mirabel, P. Solubility of Polyvalent Cations in Fogwater at an Urban Site in Strasbourg (France). *Atmos. Environ.* **1995**, *29*, 2625–2631. [[CrossRef](#)]
23. Millet, M.; Sanusi, A.; Wortham, H. Chemical Composition of Fogwater in an Urban Area: Strasbourg (France). *Environ. Pollut.* **1996**, *94*, 345–354. [[CrossRef](#)]
24. Millet, M.; Wortham, H.; Sanusi, A.; Mirabel, P. Low Molecular Weight Organic Acids in Fogwater in an Urban Area: Strasbourg (France). *Sci. Total Environ.* **1997**, *206*, 57–65. [[CrossRef](#)]
25. Millet, M. Etude de la Composition Chimique des Brouillards et Analyse des Pesticides dans les Phases Liquide, Gazeuse et particulaire de Atmosphere. Ph.D. Thesis, Université Louis Pasteur, Strasbourg, France, 1994; 204p.
26. Asif, M.; Yadav, R.; Sughra, A.; Bhatti, M.S. Chemical Composition and Source Apportionment of Winter Fog in Amritsar: An Urban City of North-Western India. *Atmosphere* **2022**, *13*, 1376. [[CrossRef](#)]
27. Khoury, D.; Millet, M.; Jabali, Y.; Delhomme, O. Occurrence of Polycyclic Aromatic Hydrocarbons and Polychlorinated Biphenyls in Fogwater at Urban, Suburban, and Rural Sites in Northeast France between 2015 and 2021. *Atmosphere* **2024**, *15*, 291. [[CrossRef](#)]
28. Demoz, B.B.; Collett, J.L.; Daube, B.C. On the Caltech Active Strand Cloudwater Collectors. *Atmos. Res.* **1996**, *41*, 47–62. [[CrossRef](#)]
29. Daube, B.C., Jr.; Flagan, R.C.; Hoffmann, M.R. California Institute of Technology CalTech. Active Cloudwater Collector. U.S. Patent 4,697,462, 6 October 1987.
30. Khoury, D.; Millet, M.; Weissenberger, T.; Delhomme, O.; Jabali, Y. Chemical Composition of Fogwater Collected at Four Sites in North- and Mount-Lebanon during 2021. *Atmos. Pollut. Res.* **2024**, *15*, 101958. [[CrossRef](#)]
31. Danielsson, L.G. On the Use of Filters for Distinguishing between Dissolved and Particulate Fractions in Natural Waters. *Water Res.* **1982**, *16*, 179–182. [[CrossRef](#)]
32. Herckes, P.; Lee, T.; Trenary, L.; Kang, G.; Chang, H.; Collett, J.L. Organic Matter in Central California Radiation Fogs. *Environ. Sci. Technol.* **2002**, *36*, 4777–4782. [[CrossRef](#)]
33. Morales, J.A.; Pirela, D.; De Nava, M.G.; De Borrego, B.S.; Velásquez, H.; Durán, J. Inorganic Water Soluble Ions in Atmospheric Particles over Maracaibo Lake Basin in the Western Region of Venezuela. *Atmos. Res.* **1998**, *46*, 307–320. [[CrossRef](#)]
34. Lu, C.; Niu, S.; Tang, L.; Lv, J.; Zhao, L.; Zhu, B. Chemical Composition of Fog Water in Nanjing Area of China and Its Related Fog Microphysics. *Atmos. Res.* **2010**, *97*, 47–69. [[CrossRef](#)]
35. Watanabe, K.; Takebe, Y.; Sode, N.; Igarashi, Y.; Takahashi, H.; Dokiya, Y. Fog and Rain Water Chemistry at Mt. Fuji: A Case Study during the September 2002 Campaign. *Atmos. Res.* **2006**, *82*, 652–662. [[CrossRef](#)]
36. Warneck, P.; Williams, J. The Atmospheric Aerosol. In *The Atmospheric Chemist's Companion*; Springer: Dordrecht, The Netherlands, 2012; pp. 127–187. [[CrossRef](#)]
37. Possanzini, M.; Buttini, P.; Di Palo, V. Characterization of a Rural Area in Terms of Dry and Wet Deposition. *Sci. Total Environ.* **1988**, *74*, 111–120. [[CrossRef](#)]
38. Di Girolamo, L.; Bond, T.C.; Bramer, D.; Diner, D.J.; Fetting, F.; Kahn, R.A.; Martonchik, J.V.; Ramana, M.V.; Ramanathan, V.; Rasch, P.J. Analysis of Multi-angle Imaging SpectroRadiometer (MISR) Aerosol Optical Depths over Greater India during Winter 2001–2004. *Geophys. Res. Lett.* **2004**, *31*, 23115. [[CrossRef](#)]
39. Yadav, S.; Kumar, P. Pollutant Scavenging in Dew Water Collected from an Urban Environment and Related Implications. *Air Qual. Atmos. Health* **2014**, *7*, 559–566. [[CrossRef](#)]
40. Tsurut, H. Acid precipitation in Eastern Asia. *Kagaku* **1989**, *59*, 305–315.
41. Błaś, M.; Polkowska, Z.; Sobik, M.; Klimaszewska, K.; Nowiński, K.; Namieśnik, J. Fog Water Chemical Composition in Different Geographic Regions of Poland. *Atmos. Res.* **2010**, *95*, 455–469. [[CrossRef](#)]
42. Hara, H.; Kitamura, M.; Mori, A.; Noguchi, I.; Ohizumi, T.; Seto, S.; Takeuchi, T.; Deguchi, T. Precipitation Chemistry in Japan 1989–1993. *Water Air Soil Pollut.* **1995**, *85*, 2307–2312. [[CrossRef](#)]
43. Islam, M.F.; Majumder, S.S.; Mamun, A.A.; Khan, M.B.; Rahman, M.A.; Salam, A. Trace Metals Concentrations at the Atmosphere Particulate Matters in the Southeast Asian Mega City (Dhaka, Bangladesh). *OJAP* **2015**, *04*, 86–98. [[CrossRef](#)]
44. Yaroshevsky, A.A. Abundances of Chemical Elements in the Earth's Crust. *Geochem. Int.* **2006**, *44*, 48–55. [[CrossRef](#)]
45. Waldman, J.M.; Munger, J.W.; Jacob, D.J.; Hoffmann, M.R. Chemical Characterization of Stratus Cloudwater and Its Role as a Vector for Pollutant Deposition in a Los Angeles Pine Forest. *Tellus B Chem. Phys. Meteorol.* **1985**, *37*, 91. [[CrossRef](#)]
46. Watanabe, K.; Ji, J.; Harada, H.; Sunada, Y.; Honoki, H. Recent Characteristics of Fog Water Chemistry at Mt. Tateyama, Central Japan: Recovery from High Sulfate and Acidity. *Water Air Soil. Pollut.* **2022**, *233*, 300. [[CrossRef](#)]
47. Nahar, K.; Nahian, S.; Jeba, F.; Islam, M.S.; Rahman, M.S.; Choudhury, T.R.; Fatema, K.J.; Salam, A. Characterization and Source Discovery of Wintertime Fog on Coastal Island, Bangladesh. *Atmosphere* **2022**, *13*, 497. [[CrossRef](#)]
48. Ambade, B. Characterization and Source of Fog Water Contaminants in Central India. *Nat. Hazards* **2014**, *70*, 1535–1552. [[CrossRef](#)]
49. Michna, P.; Werner, R.A.; Eugster, W. Does Fog Chemistry in Switzerland Change with Altitude? *Atmos. Res.* **2015**, *151*, 31–44. [[CrossRef](#)]

50. Raja, S.; Ravikrishna, R.; Kommalapati, R.R.; Valsaraj, K.T. Monitoring of Fogwater Chemistry in the Gulf Coast Urban Industrial Corridor: Baton Rouge (Louisiana). *Env. Monit. Assess.* **2005**, *110*, 99–120. [[CrossRef](#)] [[PubMed](#)]
51. Fisak, J.; Tesar, M.; Rezacova, D.; Elias, V.; Weignerova, V.; Fottova, D. Pollutant Concentrations in Fog and Low Cloud Water at Selected Sites of the Czech Republic. *Atmos. Res.* **2002**, *64*, 75–87. [[CrossRef](#)]
52. Raja, S.; Raghunathan, R.; Yu, X.-Y.; Lee, T.; Chen, J.; Kommalapati, R.R.; Murugesan, K.; Shen, X.; Qingzhong, Y.; Valsaraj, K.T.; et al. Fog Chemistry in the Texas–Louisiana Gulf Coast Corridor. *Atmos. Environ.* **2008**, *42*, 2048–2061. [[CrossRef](#)]
53. Cardito, A.; Carotenuto, M.; Amoroso, A.; Libralato, G.; Lofrano, G. Air quality trends and implications pre and post COVID-19 restrictions. *Sci. Total Environ.* **2023**, *879*, 162833. [[CrossRef](#)]
54. Khan, S.; Dahu, B.M.; Scott, G.J. A Spatio-temporal Study of Changes in Air Quality from Pre-COVID Era to Post-COVID Era in Chicago, USA. *Aerosol Air Qual. Res.* **2022**, *22*, 220053. [[CrossRef](#)]
55. Straub, D.J.; Hutchings, J.W.; Herckes, P. Measurements of Fog Composition at a Rural Site. *Atmos. Environ.* **2012**, *47*, 195–205. [[CrossRef](#)]
56. Salem, T.A.; Omar, M.E.D.M.; El Gammal, H.A.A. Evaluation of Fog and Rain Water Collected at Delta Barrage, Egypt as a New Resource for Irrigated Agriculture. *J. Afr. Earth Sci.* **2017**, *135*, 34–40. [[CrossRef](#)]
57. Ehrenhauser, F.S.; Khadapkar, K.; Wang, Y.; Hutchings, J.W.; Delhomme, O.; Kommalapati, R.R.; Herckes, P.; Wornat, M.J.; Valsaraj, K.T. Processing of Atmospheric Polycyclic Aromatic Hydrocarbons by Fog in an Urban Environment. *J. Environ. Monit.* **2012**, *14*, 2566. [[CrossRef](#)]
58. Raja, S.; Raghunathan, R.; Kommalapati, R.R.; Shen, X.; Collett, J.L.; Valsaraj, K.T. Organic Composition of Fogwater in the Texas–Louisiana Gulf Coast Corridor. *Atmos. Environ.* **2009**, *43*, 4214–4222. [[CrossRef](#)]
59. Collett, J.L.; Herckes, P.; Youngster, S.; Lee, T. Processing of Atmospheric Organic Matter by California Radiation Fogs. *Atmos. Res.* **2008**, *87*, 232–241. [[CrossRef](#)]
60. Fuzzi, S.; Facchini, M.C.; Decesari, S.; Matta, E.; Mircea, M. Soluble Organic Compounds in Fog and Cloud Droplets: What Have We Learned over the Past Few Years? *Atmos. Res.* **2002**, *64*, 89–98. [[CrossRef](#)]
61. Decesari, S.; Facchini, M.C.; Fuzzi, S.; Tagliavini, E. Characterization of Water-soluble Organic Compounds in Atmospheric Aerosol: A New Approach. *J. Geophys. Res.* **2000**, *105*, 1481–1489. [[CrossRef](#)]
62. Facchini, M.C.; Fuzzi, S.; Zappoli, S.; Andracchio, A.; Gelencsér, A.; Kiss, G.; Krivácsy, Z.; Mészáros, E.; Hansson, H.; Alsberg, T.; et al. Partitioning of the Organic Aerosol Component between Fog Droplets and Interstitial Air. *J. Geophys. Res.* **1999**, *104*, 26821–26832. [[CrossRef](#)]
63. Collett, J. Internal Acid Buffering in San Joaquin Valley Fog Drops and Its Influence on Aerosol Processing. *Atmos. Environ.* **1999**, *33*, 4833–4847. [[CrossRef](#)]
64. Aleksic, N.; Dukett, J.E. Probabilistic Relationship between Liquid Water Content and Ion Concentrations in Cloud Water. *Atmos. Res.* **2010**, *98*, 400–405. [[CrossRef](#)]
65. Elbert, W.; Krämer, M.; Andreae, M.O. Reply to Discussion on Control of Solute Concentrations in Cloud and Fog Water by Liquid Water Content. *Atmos. Environ.* **2002**, *36*, 1909–1910. [[CrossRef](#)]
66. Cuhadaroglu, B.; Demirci, E. Influence of Some Meteorological Factors on Air Pollution in Trabzon City. *Energy Build.* **1997**, *25*, 179–184. [[CrossRef](#)]
67. Klimont, Z.; Cofala, J.; Schöpp, W.; Amann, M.; Streets, D.G.; Ichikawa, Y.; Fujita, S. Projections of SO<sub>2</sub>, NO<sub>x</sub>, NH<sub>3</sub> and VOC emissions in East Asia up to 2030. *Water Air Soil Pollut.* **2001**, *130*, 193–198. [[CrossRef](#)]
68. Chatain, M.; Chretien, E.; Crunaire, S.; Jantzem, E. Road Traffic and Its Influence on Urban Ammonia Concentrations (France). *Atmosphere* **2022**, *13*, 1032. [[CrossRef](#)]
69. Ohara, T.; Akimoto, H.; Kurokawa, J.; Horii, N.; Yamaji, K.; Yan, X.; Hayasaka, T. An Asian Emission Inventory of Anthropogenic Emission Sources for the Period 1980–2020. *Atmos. Chem. Phys.* **2007**, *7*, 4419–4444. [[CrossRef](#)]
70. Collett, J.L.; Bator, A.; Sherman, D.E.; Moore, K.F.; Hoag, K.J.; Demoz, B.B.; Rao, X.; Reilly, J.E. The Chemical Composition of Fogs and Intercepted Clouds in the United States. *Atmos. Res.* **2002**, *64*, 29–40. [[CrossRef](#)]
71. Shen, Z.; Arimoto, R.; Cao, J.; Zhang, R.; Li, X.; Du, N.; Okuda, T.; Nakao, S.; Tanaka, S. Seasonal Variations and Evidence for the Effectiveness of Pollution Controls on Water-Soluble Inorganic Species in Total Suspended Particulates and Fine Particulate Matter from Xi’an, China. *J. Air Waste Manag. Assoc.* **2008**, *58*, 1560–1570. [[CrossRef](#)]
72. Zhang, Q.; Shen, Z.; Cao, J.; Zhang, R.; Zhang, L.; Huang, R.-J.; Zheng, C.; Wang, L.; Liu, S.; Xu, H.; et al. Variations in PM<sub>2.5</sub>, TSP, BC, and Trace Gases (NO<sub>2</sub>, SO<sub>2</sub>, and O<sub>3</sub>) between Haze and Non-Haze Episodes in Winter over Xi’an, China. *Atmos. Environ.* **2015**, *112*, 64–71. [[CrossRef](#)]
73. Nieberding, F.; Breuer, B.; Braeckvelt, E.; Klemm, O.; Song, Q.; Zhang, Y. Fog Water Chemical Composition on Ailaoshan Mountain, Yunnan Province, SW China. *Aerosol Air Qual. Res.* **2018**, *18*, 37–48. [[CrossRef](#)]
74. Wang, Y.; Guo, J.; Wang, T.; Ding, A.; Gao, J.; Zhou, Y.; Collett, J.L.; Wang, W. Influence of Regional Pollution and Sandstorms on the Chemical Composition of Cloud/Fog at the Summit of Mt. Taishan in Northern China. *Atmos. Res.* **2011**, *99*, 434–442. [[CrossRef](#)]
75. Munger, J.W.; Jacob, D.J.; Waldman, J.M.; Hoffmann, M.R. Fogwater Chemistry in an Urban Atmosphere. *J. Geophys. Res.* **1983**, *88*, 5109–5121. [[CrossRef](#)]
76. Ali, K.; Momin, G.A.; Tiwari, S.; Safai, P.D.; Chate, D.M.; Rao, P.S.P. Fog and Precipitation Chemistry at Delhi, North India. *Atmos. Environ.* **2004**, *38*, 4215–4222. [[CrossRef](#)]

- 
77. Gelencsér, A.; Sallai, M.; Krivácsy, Z.; Kiss, G.; Mészáros, E. Voltammetric Evidence for the Presence of Humic-like Substances in Fog Water. *Atmos. Res.* **2000**, *54*, 157–165. [[CrossRef](#)]
  78. Fisak, J.; Stoyanova, V.; Tesar, M.; Petrova, P.; Daskalova, N.; Tsacheva, T.; Marinov, M. The Pollutants in Rime and Fog Water and in Air at Milesovka Observatory (Czech Republic). *Biologia* **2009**, *64*, 492–495. [[CrossRef](#)]

**Disclaimer/Publisher’s Note:** The statements, opinions and data contained in all publications are solely those of the individual author(s) and contributor(s) and not of MDPI and/or the editor(s). MDPI and/or the editor(s) disclaim responsibility for any injury to people or property resulting from any ideas, methods, instructions or products referred to in the content.